

FLUID DISTRIBUTION IN TRANSITION ZONES (Using a New Initial-Residual Saturation Correlation)

M.Sarwaruddin¹, A. Skauge² and O. Torsæter¹

¹Norwegian University of Science & Technology, ²Norsk Hydro

ABSTRACT

The fluid distribution as a function of height in transition zones is often very complex. This may be due to movement of water-oil contact, tilting of the reservoir at some point in time, leak of fluid out of the reservoir zone or complex inflow during secondary migration. The resultant fluid distribution seen in saturation logs may be difficult to model. In this paper we address the changes in fluid distribution versus height, inferred by changes of fluid distribution due to the movement of water-oil contact only.

The experimental procedures for determining capillary pressure are based on fluid saturation monitoring by gamma absorption from centrifuge experiments. An analytical capillary pressure-saturation model was fit to the bounding imbibition capillary pressure-saturation data. The drainage-imbibition hysteresis curves were then constructed assuming that these curves have similar shape to that of the bounding imbibition curve. The imbibition hysteresis model proposed may be used to calculate fluid saturation in the reservoir due to the movement of water-oil contact. We also proposed necessary auxiliary equations to solve the new linear and four-parameter (sigmoidal type) initial-residual fluid saturation equations. Thus once the shape of the bounding-imbibition capillary pressure-saturation curve and maximum non-wetting fluid saturation are known one can easily construct any imbibition hysteresis curves that may be required.

INTRODUCTION

The potential and importance of transition zones are discussed in a number of recent and old papers¹⁻⁵. Oil transition zone is a zone above the water-oil contact where the water saturation (S_w) is above the irreducible water saturation. In many cases recovery from transition zones are not economical, however for a low permeability reservoir, entire reservoir or a substantial part of it might become a potential target for recovery.

In this paper, we present a new initial (S_{nwi}) -residual (S_{nwr}) non-wetting fluid correlation that can be used to construct imbibition capillary pressure (P_c) hysteresis curves. No attempt has been made to model imbibition relative permeability (k_{ro}/k_{rw}) curves. However if no data is available, a first estimate can be obtained by using Corey-Burdine⁶ correlation. No data has been collected for secondary drainage. Further capillary pressure hysteresis has been reported⁷⁻⁹ to be a closed loop type hysteresis curves. Tan¹⁰ notes that Killough's P_c hysteresis model¹² is suitable for specific reservoir types where the imbibition and drainage curves meet at the same residual (non-wetting) fluid saturation. Kleppe *et al*¹¹ criticised the formulation of Killough's model since it is based on Land's¹³ initial-residual non-wetting fluid correlation.

Using limited experimental data and synthetic core, Kleppe *et al* showed that a linear correlation exists between S_{nwi} and S_{nwr} . Masalmeh and Oedai² also found piecewise linear-constant correlation between S_{nwi} and S_{nwr} for low permeable carbonate samples. Fanchi *et al*³ reported experimental data on 20/40-70/100 mesh glass beads that showed a kind of S-shaped relation between S_{nwi} and S_{nwr} . Based on experimental investigation Larsen *et al*¹ concluded that Land's S_{nwi} - S_{nwr} correlation predicts too high S_{nwr} at low values of S_{nwi} . Morrow and Harris¹⁴ also confirmed this and their experimental Pc hysteresis curves suggest that Killough's model might be suitable for unconsolidated sand but most likely will fail for consolidated material.

THE EXPERIMENTAL PROCEDURES AND DATA PROCESSING

Using centrifuge (Beckman L8-55/P), high melting point ($29^0 \sim 32^0$ C) paraffin oil ($C_{19}H_{40}$) and gamma absorption technique similar to Sarwaruddin^{16,17} approach, we have been able to establish, maintain and calculate fluid distribution profile for liquid-wet Berea cores. The standard deviation of each saturation value was estimated to 0.01 saturation fraction after setting γ -ray counting time to 20 minutes^{18, 19}. Note that radial and gravity effect^{20, 21} was considered when average Pc was related to the corresponding average saturation.

According to the above procedures, we gathered a set of $\{\bar{S}_w, \bar{P}_c\}$ of data points for three samples (Sample ID: Bx3, Bx4 and Bx5). For each sample, a non-linear regression was performed to smooth the data points using a weighting factor $1/\bar{P}_c^2$ and a constraint $S_{wir} \leq \bar{S}_w^{\min}$. Here S_{wir} is referred as irreducible wetting fluid saturation, while \bar{S}_w^{\min} as minimum measured average saturation at any cross-section of a given sample. We used Microsoft® Excel's solver function to minimise the $\sum(1 - \bar{P}_{c,a}/\bar{P}_c)^2$. Here, $\bar{P}_{c,a}$ is analytical Pc of the following form

$$\bar{P}_{c,a} = a \left(\frac{\bar{S}_w - S_{wir}}{1 - S_{wir}} \right)^{-n} \quad \dots(1)$$

In Eq.3, "a", "n" and S_{wir} are fitting parameters and their values are determined by regression. The best-fit analytical Pc-saturation function was used to estimate initial fluid distribution in the transition zone. The movement of water-oil contact reduces the capillary pressure at every point along the height of the transition zone. The reduction of Pc also changes the fluid saturation that may be obtained from a set of similar but different imbibition Pc-saturation curves (see Fig.1), if the reservoir in question is water-wet. The imbibition Pc curves are also called hysteresis curves and note that each of them satisfies their turning/initial wetting fluid saturation (S_{wi}) point.

In this experiment, the movement of water-oil contact is simulated changing the liquid level in the centrifugation cup. After rising the liquid level, the centrifuge is again run at a set rotation. This procedures allows us to collect a large pair of initial-final fluid saturation data $\{S_{wi}, S_{wr}\}$ which are basically end point data for the drainage-imbibition Pc hysteresis curves. Note that we regard a point in the sample reached to the residual saturation only if its \bar{P}_c value reached -5 kPa, which is approximately -10 kPa for an equivalent water-oil system. The bounding imbibition curves were also obtained after establishment of

irreducible liquid saturation (S_{wir}) and each of the curves was fit to an imbibition Pc model shown below

$$P_c^I(S_w) = \frac{C_1}{(S_w - S_{w1})^{n_1}} - \frac{C_2}{(S_{w2} - S_w)^{n_2}}; \quad S_{wir} \leq S_w \leq (1 - S_{nwr}^{\max}) \quad \dots(2)$$

Here, $P_c^I(S_w)$: Imbibition Pc, a function S_w , S_w : Wetting fluid saturation; C_1, C_2 are positive constants; n_1, n_2 are exponents and S_{w1}, S_{w2} are two asymptotes. Note that for bounding imbibition Pc, $S_{w1} \leq S_{wir}$, S_{wir} : irreducible wetting fluid saturation and $S_{w2} \geq 1 - S_{nwr}^{\max}$, S_{nwr}^{\max} : maximum residual non-wetting fluid saturation.

In order to construct drainage-imbibition Pc hysteresis curves, we collected some experimental drainage-imbibition Pc-saturation data including end point data $\{S_{wi}, S_{wr}\}$ sets for the above samples. The imbibition Pc model (Eq.2) is again used to fit the data. However, for each drainage-imbibition curve, the asymptotes $\{S_{w1}, S_{w2}\}$ were determined honouring the corresponding initial-residual set $\{S_{wi}, S_{wr}\}$. Except "n₂", the bounding shape parameters i.e. C_1, C_2 and n_1, n_2 are assumed to be equal for all other drainage-imbibition hysteresis curves. The exponent "n₂" has been used to adjust the shape of the hysteresis curves from that of the bounding imbibition curve. We recommend adjusting n_2 as a linear function of S_{nwi} . For the three samples that were used in this experiment, the average slope was found 0.43 while the intercept at $S_{nwi}=0$, may be obtained honouring the bounding n_2 . Note that saturation boundary for the hysteresis curves (Eq.2) are $S_{wi} \leq S_w \leq S_{wr}$ although difference between the asymptotes S_{w1}, S_{w2} is larger than S_{wi} and S_{wr} .

THE NEW INITIAL-RESIDUAL SATURATION CORRELATION

Using the experimental procedures discussed earlier, a large number of data set $\{S_{wi}, S_{wr}\}$ has been collected for four Berea samples (Bx2, Bx3, Bx4 and Bx5) whose average porosity and permeability are 22.6% and 228 md respectively. The corresponding initial-residual non-wetting fluid saturation (S_{nwi}, S_{nwr}) is plotted for these samples in Fig2. Linear and sigmoidal equations of the following form are fitted to the data by non-linear regression tool.

$$S_{nwr} = (m)S_{nwi} \quad ; \quad S_{nwi}^* > S_{nwi} \geq 0 \quad \dots(3a)$$

Where, m and S_{nwi}^* are constants. The slope "m" is estimated to be equal to 0.15 while S_{nwi}^* may be determined solving Eq.3a and Eq.3b. There might have several solutions for S_{nwi}^* , however, we suggest taking the minimum S_{nwi}^* . In case, no solution is found for S_{nwi}^* , one may seek a solution by slightly increasing the value of "m".

$$S_{nwr} = Y_0 + \frac{b}{1 + e^{-(S_{nwi} - S_{nwo})/d}} \quad ; \quad 1 \geq S_{nwi} \geq S_{nwi}^* \quad \dots(3b)$$

Where, Y_0, b, d and S_{nwo} are fitting parameters.

Apparently Eq.3b is bit complicated since it involves four parameters which are difficult to obtain. However a closer look to Eq.3b reveals that "d" is simply a scaling parameter

which ensures that the denominator $[1+e^{-(S_{nwi}-S_{nwo})/d}]$ becomes ≈ 1 as S_{nwi} equals to $(1-S_{wir})$. Therefore, parameter "b" becomes S_{nwr}^{\max} the maximum residual non-wetting fluid saturation.

Accordingly "d" may be estimated from a functional relation such that $d = f_2(b \equiv S_{nwr}^{\max})$. The other parameters S_{nwo} and Y_0 may be considered as a rock-fluid property of porous media. Hence it is also expected that S_{nwo} and Y_0 may be written as $S_{nwo} = f_1(S_{nwr}^{\max})$ and $Y_0 = Y_0(S_{nwr}^{\max})$ since S_{nwr}^{\max} is a rock-fluid property. Considering the arguments above, equation 3b can be rewritten as

$$S_{nwr} = Y_0(S_{nwr}^{\max}) + \frac{S_{nwr}^{\max}}{1 + e^{-(S_{nwi} - f_1(S_{nwr}^{\max})/f_2(S_{nwr}^{\max}))}} \quad \dots(4a)$$

With the regressed parameters obtained from Fig2, we found the following functions for $f_1(S_{nwr}^{\max})$ and $f_2(S_{nwr}^{\max})$ and Y_0 .

$$f_1(S_{nwr}^{\max}) = 0.7223 S_{nwr}^{\max} + 0.1815 \quad \dots(4b)$$

$$f_2(S_{nwr}^{\max}) = 0.096 S_{nwr}^{\max} + 0.0432 \quad \dots(4c)$$

$$Y_0 = 0.0218 S_{nwr}^{\max} - 0.0014 \quad \dots(4d)$$

Now, Eq.3a and 4a can be solved using equation 4b, 4c and 4d if one has knowledge about S_{nwr}^{\max} either from experimental bounding imbibition curve or from other sources.

RESULTS AND DISCUSSION

The initial fluid distribution in the transition zone was modelled by primary drainage Pc-saturation function. The drainage Pc function was obtained in two stages. In order to capture saturation at low Pc range, we conducted centrifuge experiment at 500 rpm while data was extended to high Pc range during drainage-imbibition experiment at 1000 rpm. We also conducted centrifuge experiment at 2000 rpm to establish irreducible wetting fluid saturation (S_{wir}). We fit Pc-saturation data together with the experimentally determined S_{wir} to analytical Eq.1 The analytical equation was then used as our basis for initial fluid distribution function. One of the analytical drainage Pc function (Bx3) is shown in Fig.3 for demonstration purpose.

Centrifuge experiments were conducted again at 500 rpm after the establishment of S_{wir} in order to obtain the full bounding imbibition curves (positive as well as negative part) for the three samples (Bx3, Bx4 and Bx5). The imbibition Pc model, Eq.2 was fit to the bounding imbibition Pc-saturation data. The drainage-imbibition experiments provide initial-residual wetting-fluid saturation data. The analytical drainage Pc, bounding imbibition Pc and initial-residual wetting fluid saturation data and some experimental hysteresis data are gathered. However, for page limitation, one sample-Bx3 is drawn in Fig4. The drainage-imbibition hysteresis curves are also shown in Fig4.

Fig.5 is a comparison between our new initial-residual non-wetting saturation model to the other existing models i.e. from Land¹³, Kleppe¹¹, Masalmeh² and Jerauld²³. In order to compare the different models, we choose the sample Bx3 and its properties i.e. $S_{mvr}^{\max}=0.2$, $S_{mvi}^{\max}=0.84$ from the bounding Pc imbibition curve.

CONCLUSIONS

A new initial-residual non-wetting-fluid-saturation correlation has been proposed which may be used for calculating fluid saturation distribution in transition zone due to the movement of water-oil contact.

REFERENCES

1. Larsen, J.A., Thorsen, T. and Haaskjold, G.: "Capillary Transition Zones from a Core Analysis perspective" Paper SCA 2000-20, 2000, Abu Dhabi, UAE.
2. Masalmeh, S. and Oedai, S.: "Oil Mobility in Transition Zones" Paper SCA 2000-02, 2000, Abu Dhabi, UAE.
3. Fanchi, J.R., Christiansen, R.L. and Heymans, M.J.: "An Improved Method for Estimating Oil reserves in Oil/Water Transitions Zones" Paper SPE 59352, Oklahoma, 3-5 April 2000.
4. Christiansen, R.L., Heymans, M.J. and Kumar, A.: "Transition Zone Characterization with Appropriate Rock-fluid Property Measurements", Paper SCA9939, 1999, Colorado, USA.
5. Eigestad, G.T. and Larsen, J.A.: "Numerical Modelling of Capillary Transition Zones", Paper SPE 64374, Brisbane, Australia, 16-18 Oct. 2000.
6. Burdine, N.T.: "Relative Permeability Calculations From Pore Size Distribution Data", Trans. AIME (1953) 198, 71-77.
7. Colonna, J., Brissaud, F., and Millet, J.L.: "Evolution of Capillarity and Relative permeability Hysteresis", SPEJ (Feb. 1972) 28-38, Trans., AIME. 253.
8. Evrenos, A.I. and Comer, A.G.: "Numerical Simulation of Hysteretic Flow in Porous Media", Paper SPE 2693, Denver, USA, Sep. 28-Oct. 1, 1969.
9. Skjæveland, S.M., Siqveland, L.M., Kjosavik, A., Hammersvold, W.L. and Virnovsky, G.A.: "Capillary Pressure Correlation for Mixed-Wet reservoirs", Paper SPE 39497, New Delhi, India, April 7-9, 1998.
10. Tan, T.: "Representation of hysteresis in capillary pressure for reservoir simulation models", *J. of Can. Pet. Tech.* (July-Aug. 1990) 29,4.
11. Kleppe, J., Hamon, G. and Chaput, E.: "Representation of Capillary Pressure Hysteresis in Reservoir Simulations", Paper SPE 38899, San Antonio, USA, 05-08 Oct. 1997.
12. Killough, J.E.: "Reservoir Simulation With History-Dependent Saturation Functions", Trans. AIME 261 (1976) 37
13. Land, C.S.: "Calculation of Imbibition Relative Permeability for Two-and Three-Phase Flow From Rock Properties", SPEJ (June 1968) 149.
14. Morrow, N.R. and Harris, C.C.: "Capillary Equilibrium in Porous Materials", Trans., AIME (1965) 234, 15-24
15. Carson, F.M.: "Simulation of Relative Permeability Hysteresis of the Nonwetting Phase", Paper SPE 10157, San Antonio, USA, 05-08 Oct. 1981.
16. Sarwaruddin, M., Torsæter, O. and Skauge, A.: "Comparing Different Methods for Capillary pressure Measurements", SCA 2000-51, 2000, Abu Dhabi, UAE.
17. Sarwaruddin, M.: "Modelling of Capillary Pressure Hysteresis by Saturation Monitoring." Ph.D. thesis, The Norwegian University of Science & Technology, Trondheim, Norway, in progress (2001).
18. Nicholls, C.I. and Heaviside, J.: "Gamma-Ray-Absorption Techniques Improve Analysis of Core Displacement Tests", Paper SPE 14421, SPE Formation Evaluation, March 1988, 69-75
19. Knoll, G. F.: "Radiation Detection and Measurement", John Wiley & Sons (1989) Second ed., 80-88
20. Hassler, G.L. and Brunner, E.: "Measurement of Capillary Pressures in Small Samples, Trans., AIME (1945) 160, 114-123

21. Forbes, P.L. 1997a: "Quantitative Evaluation and Correction of Gravity Effects on Centrifuge capillary Pressure Curves", SCA 9734, Calgary, Canada, Sep. 7-10, 1997.
22. Leverett, M.C.: "Capillary Behaviour in Porous solids", Trans. AIME (1941) 142, 152-168
23. Jerauld, G.R. "Gas-Oil Relative Permeability of Prudhoe Bay" Paper SPE 35718, Anchorage USA, 22-24 May, 1996

NOMENCLATURE

Constants

- a = Capillary entry pressure [kPa] (Eq.1)
- C_1, C_2, n_1, n_2 = Shape parameters (Eq.2)
- m = slope, S_{nwi}^* (Eq.3a)
- Y_0, b, d, S_{nwo} = Trapping characteristic (Eq.3b)

Variables

- k_r = Relative permeability
- S = saturation
- \bar{S} = Average saturation
- P = Pressure [kPa]
- \bar{P} = Average Pressure [kPa]

Subscript:

- a = analytical, C = capillary, g = gas, o = oil, w = wetting, nw = non-wetting, wc = connate water, wi = wetting initial, nwi = non-wetting initial, wr = wetting residual, nwr = non-wetting residual, w1 = asymptote-1, asymptote-2 (Eq.2).

Superscript:

- max = maximum, min = minimum; I=I mb

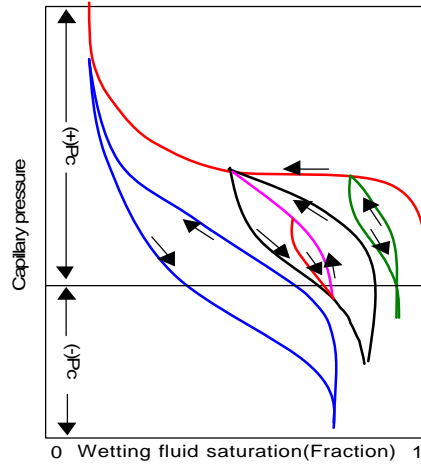


Figure 1: Imbibition Pc hysteresis curves are shown by down arrow

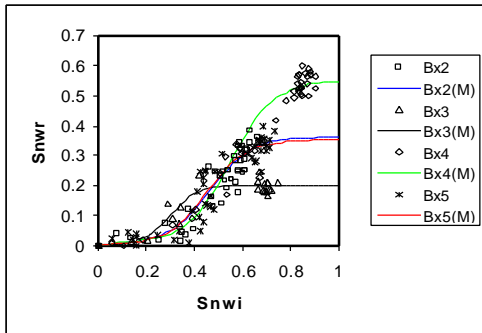


Figure 2: Initial-residual non-wetting fluid correlation. Solid lines are model equation.

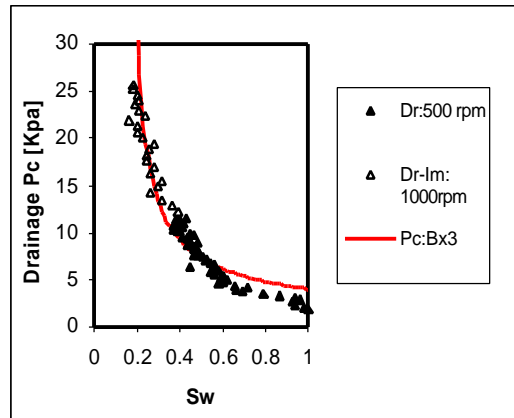


Figure 3: Best-fit drainage Pc for Bx3

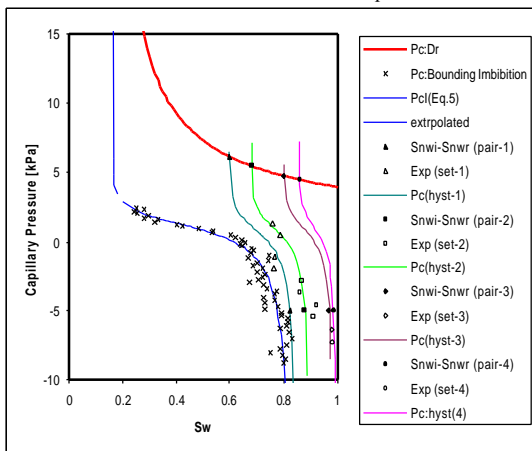


Figure 4: Bounding imbibition curve and constructed hysteresis curve together with some experimental data are shown for sample: Bx3

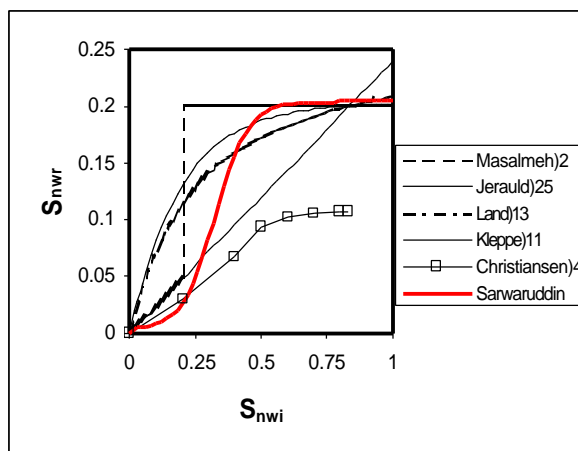


Figure 5: Comparison of different initial-residual saturation model with our proposed model